Phys. Chem. Chem. Phys., 2002, **4**(Advance Article)
DOI: 10.1039/b203686j

PCCP

Paper

Monte Carlo simulations of ion selectivity in a biological Na channel: Charge–space competition

Dezsõ Boda[a], **David D. Busath**[b], **Bob Eisenberg**[c], **Douglas Henderson**[d] **and Wolfgang Nonner***[e]

[a]*Department of Physical Chemistry, University of Veszprém, H-8201 Veszprém, P.O. Box 158, Hungary.* E-mail: boda@almos.vein.hu

[b]*Department of Zoology and Center for Neuroscience, Brigham Young University, Provo, Utah 84602.* E-mail: david_busath@byu.edu

[c]*Department of Molecular Biophysics and Physiology, Rush Medical College, Chicago, Illinois 60612.* E-mail: beisenbe@rush.edu

[d]*Department of Chemistry and Biochemistry, Brigham Young University, Provo, Utah 84602.* E-mail: doug@huey.byu.edu

[e]*Department of Physiology and Biophysics, University of Miami School of Medicine, University of Miami School of Medicine, Miami, Florida 33101.* E-mail: wnonner@chroma.med.miami.edu

Received 16th April 2002, Accepted 2nd September 2002

First published on the web 18th September 2002

Na channels that produce the action potentials of nerve and muscle include a selectivity filter formed by both positively and negatively charged amino acid residues in a molecular pore. Here we present Monte Carlo simulations of equilibrium ion absorption in such a system. Ions are treated as charged hard spheres in a uniform dielectric. Tethered carboxylate and amino groups known to line the selectivity filter of the Na channel are represented as charged hard spheres and restricted to the filter region of the channel. Consistent with experiments, we find (1) that absorption of Ca^{2+} into the filter exceeds absorption of Na^{+} only when the concentration of Ca^{2+} is some tenfold larger than physiological; (2) the model channel absorbs smaller alkali metal ions preferentially compared to larger ones. The alkali metal selectivity involves volume exclusion of larger ions from the center of the filter region.

1 Introduction

Ion channels are a major class of proteins that bridge cell membranes and thereby control many biological functions in health[1] and disease.[2] Ion channels regulate the flux of ions into the cell and, when open, select between ions. The flux is driven by the gradient of electrochemical potential, and controlled by the physical properties of the channel protein.[3] How proteins control selectivity has long been a central question in biology. Here we examine a mechanism of ion selectivity for the Na channels of nerve and muscle membranes.

Na channels are part of a large family of structurally related voltage-controlled channels that also includes Ca and K channels. The conductive pore in this family is formed between four monomers (K channels) or four homologous motifs within a single polypeptide (Na and Ca channels). The ion-selective properties of the channels seem to arise in small segments of the sequence (the 'P loop'); these segments form inserts that locally restrict the diameter of a wider pore.[4,5] Site-directed mutations suggest that the constriction in Na- and Ca-specific channels is lined by the sidechains of the amino acid residues, whereas in K channels it is lined by atoms of the polypeptide backbone.[4,6–9]

Ionic selectivities of Na and Ca channels seem largely to be determined by four residues present in corresponding positions of the four P loops. These are all glutamate (E) in Ca channels (the 'EEEE-locus'), but include aspartate (D), glutamate, lysine (K), and alanine (A) in Na channels ('DEKA-locus'). Mutating the amino acids in these four positions of the Na channel from DEKA to DEEE produces a strong shift of selectivity from Na^{+} to Ca^{2+}, in effect creating a Ca channel.[10] Further mutagenesis experiments have shown that a positively charged residue in the locus (such as lysine, arginine, or histidine at pH 6) is needed to create the low divalent affinity seen in Na channels.[11,12]

Although crystallographic coordinates of Na channels have not yet been determined, many structural properties of the pore have been deduced by other means. Hille probed the ionic pathway with protons, alkali metal cations, and organic cations, and postulated a structure for the 'selectivity filter' of the Na channel.[13,14] In this view, the selective portion is a short axial subsegment of the pore that forms a rectangular frame (aperture ≈0.3 nm × 0.5 nm) of oxygen atoms around the ionic pathway, some with charge. It is gratifying that this structural hypothesis, developed 30 years ago, seems consistent with possible arrangements of the actual primary structure, namely the DEKA locus, which was unknown and unguessed at that time, but the physical principles by which the DEKA locus produces the observed alkali metal and alkali earth selectivities remain unknown.

Recently, the physical basis of ionic selectivity in the analogous EEEE locus of Ca channels has been examined using statistical mechanics and a simple model to capture electrostatic and excluded-volume effects in the locus.[15–20] The model is a modest extension and reworking of the standard models of concentrated salt solutions found in the literature of physical chemistry in the last decade or two.[21] The four carboxylate groups in the Ca channel are represented by a cluster of 8 half-charged oxygen ions confined to a small volume (the selectivity filter) but free to move within that volume. Ca^{2+} accumulates in preference to Na^{+} or other alkali metal cations (in agreement with experiments on biological Ca channels) because of Coulombic and hard-sphere interactions among these confined oxygens and mobile ions. Ca^{2+} is preferred over Na^{+} because one divalent Ca^{2+} provides the same amount of charge as two Na^{+} in about one half the ionic volume. The crowding of charge produces selectivity because of the competition of the counterions for space, the charge–space competition (CSC) mechanism.[15,17]

This paper examines how well a CSC mechanism can account for selectivity in the DEKA locus of Na channels. We report Monte Carlo (MC) simulations of the equilibrium ion absorption that arises when Na^+ ions, other alkali metal cations, and Ca^{2+} compete in a simple representation of the DEKA locus.

2 Model

The cylindrical simulation cell is shown in Fig. 1 in an axial cross-section. The protein (excluding the charged atoms of the pore lining, see below) and lipid membrane are represented as hard walls inaccessible to ions (solid lines). Ions are reflected off the surface of these walls and cannot penetrate into the wall itself. A cylindrical hole through the protein (radius R_f, length H_f) connects two reservoirs (baths) that contain mobile ions such as Na^+, K^+, Ca^{2+}, and Cl^-. The dimensions assigned to the cylindrical hole (R_f = 0.4–0.5 nm, H_f = 1 nm) represent the narrowest part of the biological channel (the 'selectivity filter'). The baths in this simulation represent both the actual baths around the protein and the wider portions of the channel. Earlier simulations of a Ca channel showed that the inclusion of atria at either end of the pore has only small effects on ion accumulation in the filter.[19] The reflecting radial boundary of the simulation cell is far enough from the channel (R = 6.25 nm) so that edge effects can be neglected, and the axial length of the cell ($H \approx 25$ nm) is sufficient to allow ionic densities to attain bulk values. Periodic boundary conditions (pbc) are used in the axial direction, making the two baths regions of a single bath.

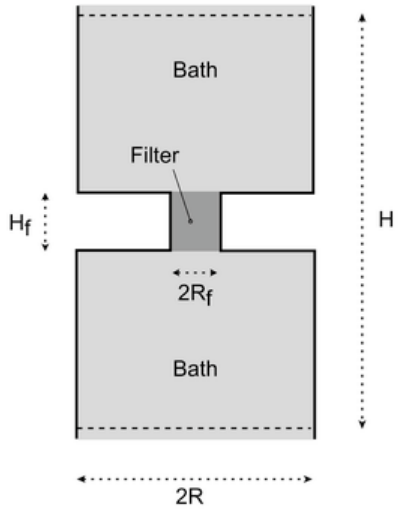

Fig. 1 Schematic diagram of the simulation cell. Ions are excluded from the membrane (including the channel protein) but not from the bath and channel. Dimensions are specified in the text.

The filter region of the Na channel contains the side chains of the DEKA locus. Two of these residues (glutamate and aspartate) carry a negatively charged carboxylate group, one residue carries a positively charged amino group (lysine), and one residue (alanine) is electrically neutral. These groups form the ends of side chains and thus are likely to have some mobility. We model these groups as 'dissolved' particles that move without restriction within the filter volume, as do mobile ions (like Na^+ or Ca^{2+}), but are confined to that volume by structural constraints (not yet specified in physical detail), following earlier work on the EEEE locus.[15–19] Note that in this description the 'filter volume' includes atoms that are part of the channel protein, *i.e.*, atoms that are covalently linked to the protein that makes the channel wall. Specifically, the two carboxylate groups are represented as four 'dissolved' half-charged oxygen ions (hard spheres of diameter 0.28 nm), the amino group is represented as a 'dissolved' ammonium ion (diameter 0.3 nm). The uncharged and short alanine residue is not represented in the model. The centers of the oxygen and ammonium ions are restricted to a subvolume of the filter so they cannot protrude from the filter. Simulations were made with the center of the ammonium ion restricted to the central 0.75 or 0.25 nm of the filter while the oxygen ions were restricted to the central 0.75 nm in all simulations.

The mobile ions are modeled as charged hard spheres with diameters 0.12 nm (Li^+), 0.19 nm (Na^+), 0.266 nm (K^+), 0.34 nm (Cs^+), 0.198 nm (Ca^{2+}), and 0.362 nm (Cl^-). The solvent is represented as a dielectric continuum (dielectric coefficient 78.5) in this so-called primitive model of electrolytes (PM). Nonner *et al.*[15,16] have used both the PM and the solvent primitive model (SPM, in which water is a solvent made of uncharged hard spheres) in computations of the Ca channel and found that the two models give qualitatively similar but quantitatively different predictions of ion accumulation (the SPM gives the same selectivities but in a smaller filter volume). A similar conclusion can be drawn from the works of Tang *et al.* who studied diffusivity and conductivity in a pore using both the PM[22] and the SPM[23] to represent the electrolyte. We start with the PM because its simulations take much less time, allowing much more exploration of conditions and alternatives.

The dielectric coefficient is assumed to be uniform everywhere (78.5) although polarization is likely to be less in the protein or lipid than it is in the aqueous baths. The assumption of a uniform dielectric coefficient is expected to reduce electrostatic effects in the filter. We accept this simplification temporarily because the polarizability of the filter region is presently unknown.

For the details of the canonical MC simulations the reader is referred to reference 19. The electrostatic effect of the periodic images in the axial direction (for which pbc's are applied) was taken into account using the charged line method.[17] The accuracy of this pbc method has been assessed.[24] An important feature of the simulation was that equilibration between the small and crowded filter and the large and dilute bath was accelerated by 'preference sampling'. In this technique, special MC steps, namely particle jumps, are performed, and the jumps that occur between the filter and the bath are given preference. The resulting bias is balanced by a factor that scales the probability of acceptance of MC steps.[19] This method has been calibrated and checked and does not introduce significant error in the domain in which we use it. Because the canonical ensemble was used, bath concentrations were an output of the simulation. Each production run was preceded by a short simulation to obtain an estimate of concentrations, followed by an adjustment of the dimension H in order to approximate the desired concentrations in the far bath. A

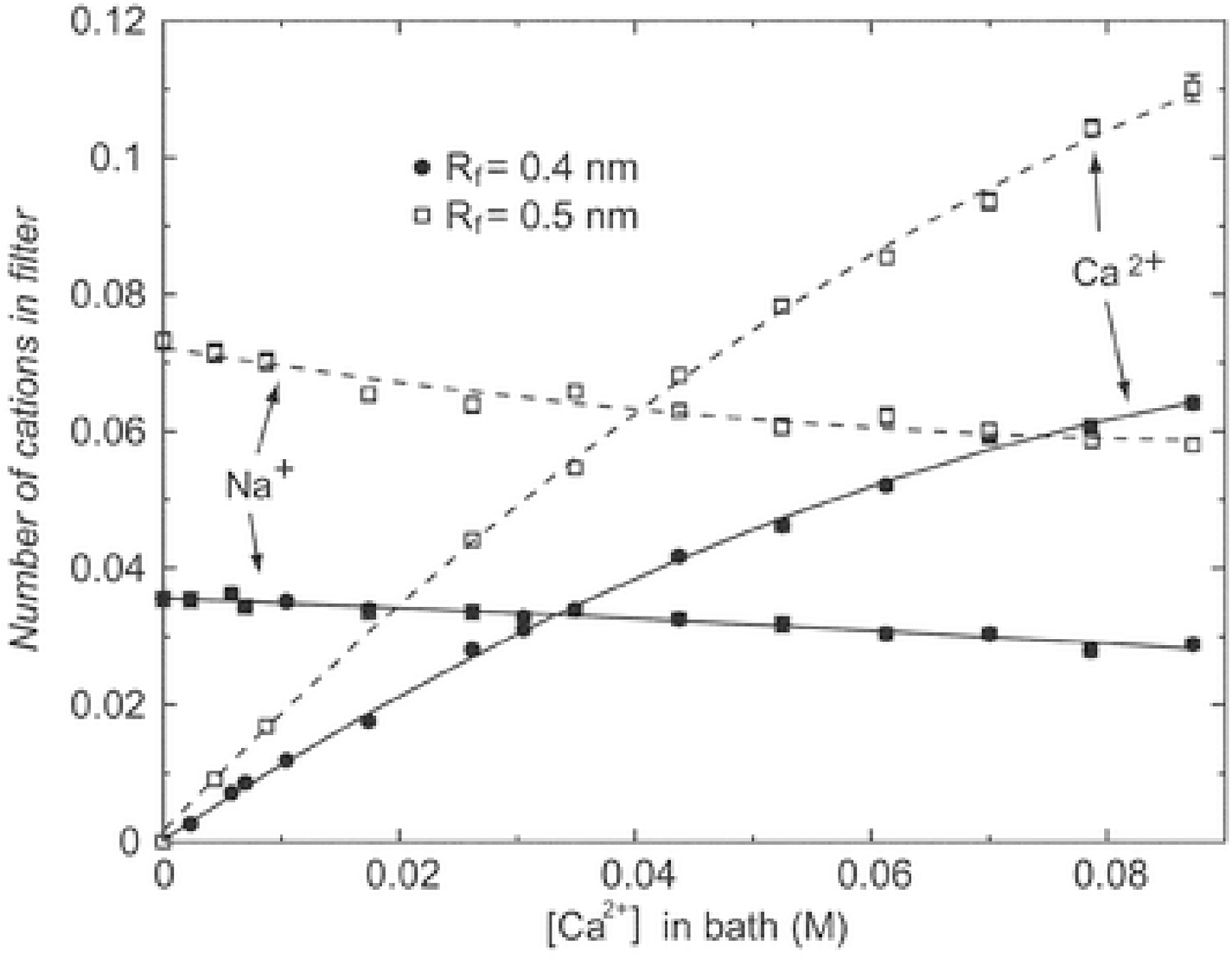

Fig. 2 Numbers of Na^+ and Ca^{2+} absorbed in the channel volume from a bath containing 0.1 M NaCl and the concentrations of $CaCl_2$ indicated on the abscissa. Simulation results (symbols) shown for two filter radii R_f. The lines are the fit used in refs. 17 and 18 and are meant only to aid the reader in connecting the symbols. The number of ions was determined by integrating ionic concentrations in the region of the filter and a 'cap' at each channel mouth that had radius R_f and extended one ionic radius in the axial direction of the bath. Note that many error bars are smaller than the symbols. The structural charge in the filter was $-e$ in all computations.

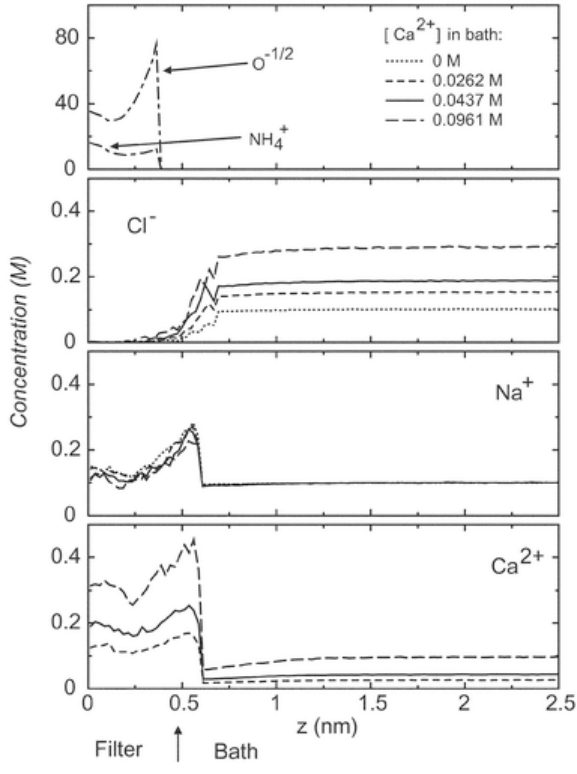

Fig. 3 Axial concentration profiles. The ordinate gives concentrations averaged over the radial coordinate $0 \leqslant r \leqslant R_f$(channel) and $0 \leqslant r \leqslant R - R_{ion}$(bath), in units of mol L^{-1}. The volume accessible to the ion centers was used for the denominator. Note that the abscissa $z = 0$ corresponds to the center of the simulation cell and channel; the profiles shown are averages of both the left and right half of the symmetrical simulation cell. The arrow marks the position of the mouth of the filter.

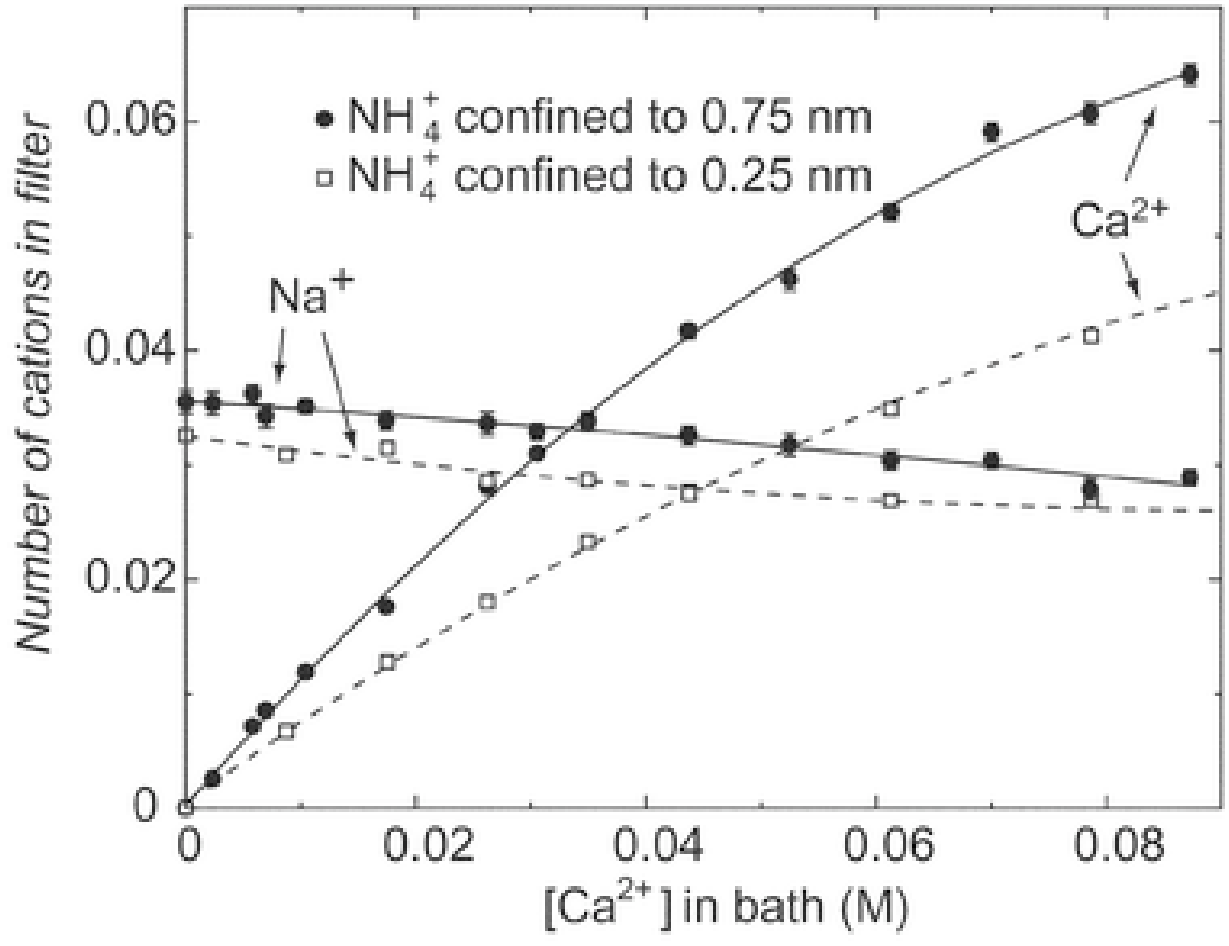

Fig. 4 Selectivity of a Na channel using a model with R_f = 0.4 nm and H_f = 1 nm for different NH_4^+ confinements. In the two sets of simulations, the NH_4^+ ion center is confined to a length of 0.375 nm and 0.125 nm on either side of the channel center, and the structural charge in the filter is –1e. The symbols give the simulation results (the lines are meant only to aid the reader in connecting the symbols).

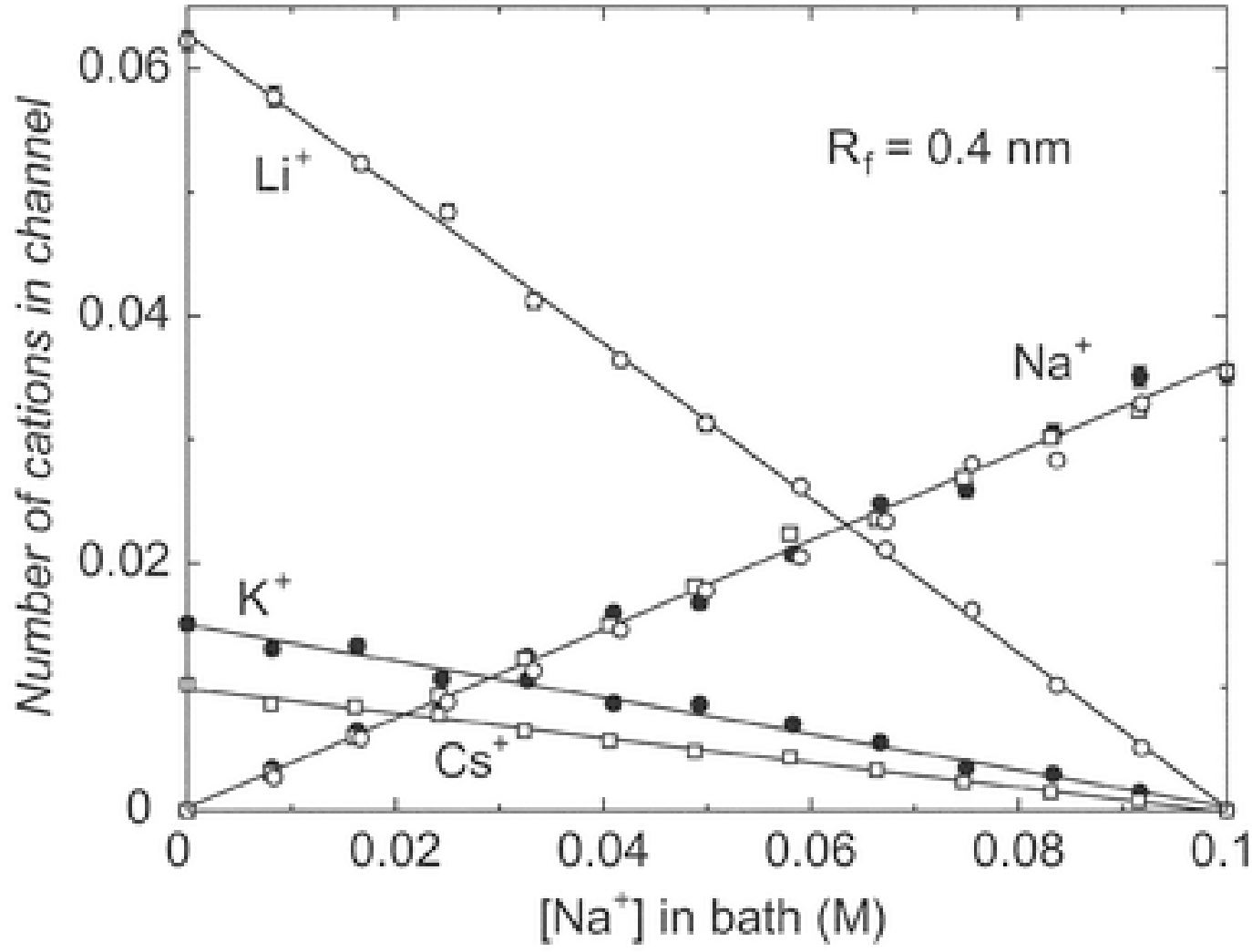

Fig. 6 Selectivity of Li^+, K^+, and Cs^+ *vs.* Na^+ in a Na channel. The filter radius in the model is R_f = 0.4 nm, and the NH_4^+ is restricted to the central 0.75 nm of the filter. The structural charge in the filter is –1e. In these simulations we start with a 0.1 M NaCl solution in the bath and gradually replace the Na^+ ions with different cations, holding the concentration of Cl^- constant at 0.1 M. The straight lines are meant only to aid the reader in connecting the points.

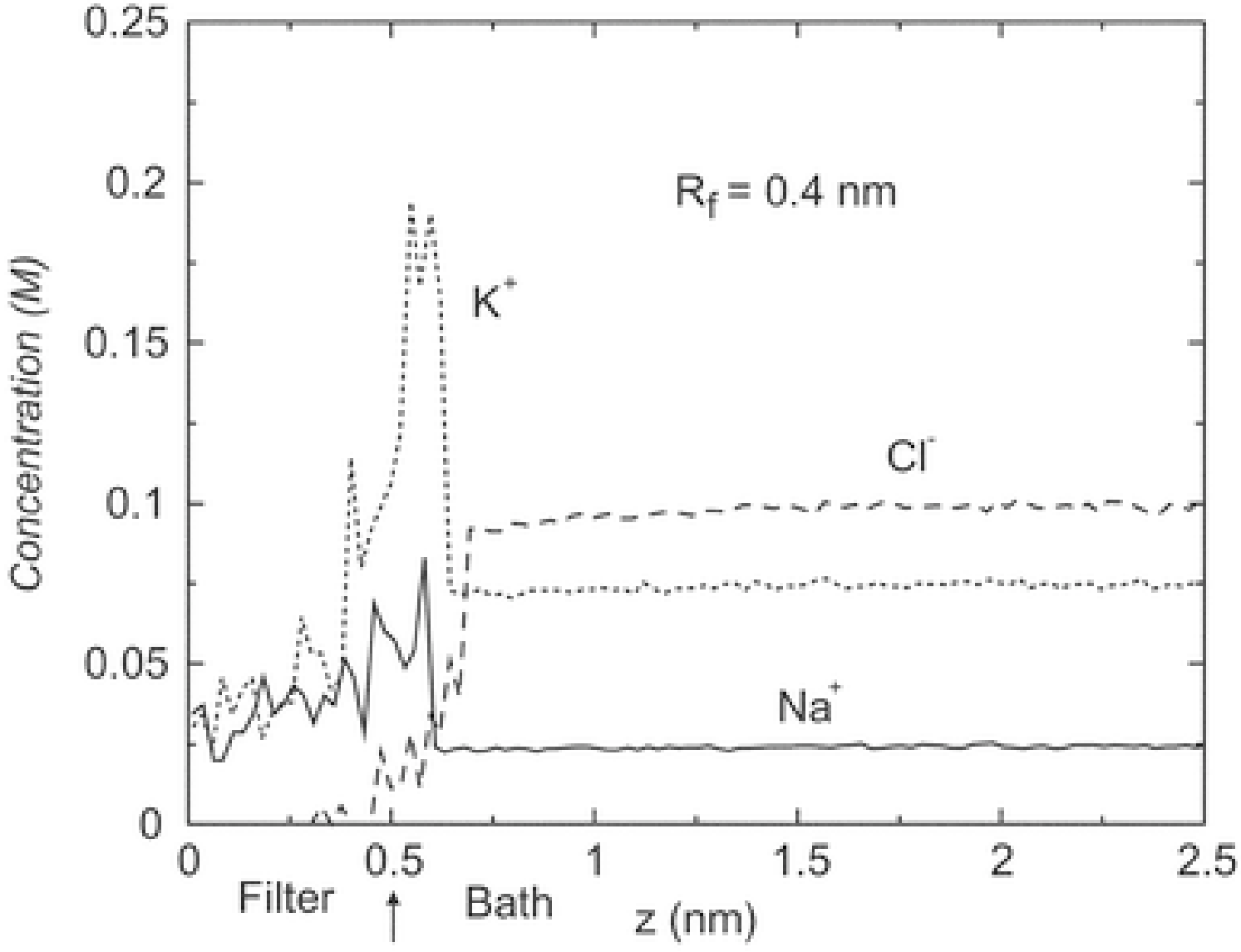

Fig. 7 Axial concentration profiles of the Na channel model with R_f = 0.4 nm. In this simulation, the bath contained a 0.1 M mixture of NaCl and KCl in the ratio ≃ 1:3. Profiles are computed as described in Fig. 3.

small ratios of pore and particle diameters. Little selectivity is observed for the diameter we assign to the Na channel ($R_f/R_{Na} \approx 4$). On the other hand, our simulations indicate substantial excluded-volume selectivity that is *repulsive* (small ions are repelled less than large ions) under these conditions. Our simulations differ from those of Goulding *et al*. because we include a high density of particle species that are restricted to the pore (the tethered oxygen and nitrogen ions) and we use a non-particulate description of water. Thus, in our model the pore contains a fluid-like density of confined and mobile ions, whereas the bath is represented as an ion gas. The asymmetry in densities is the basis of the observed repulsion of ions from the filter. This repulsion increases monotonically with ionic diameter (Fig. 6), whereas the absorption observed by Goulding *et al*. can select for either smaller or larger ions dependent on small variations of channel diameter.

Repulsive phenomena as observed in our simulations can in principle occur in two bulk phases of different particle densities and do not require a particular wall structure or channel diameter. In fact, Nonner *et al*.[15,16] have studied bulk models of a Ca channel and assessed entropic repulsive effects. In these models, water can be conveniently described in both the particulate and non-particulate models, so it is possible to assess the role of a particulate solvent. It was found that comparable repulsive selectivities can arise from excluded volume effects when appropriate filter volumes are chosen for either model: if water is described as particulate, a smaller filter volume is needed. In this case of particulate water, the confined particles in the filter are more compressed compared to calculations with non-particulate water. In both cases, there exists an asymmetry of density between the filter and bath fluids. Thus, we expect that the repulsive selectivity observed in our simulations of the Na channel would occur also when water is described as particulate, if an appropriate reduction is made to the filter volume.

It is also interesting to consider the consequences if water itself were attracted or repelled into or out of the selectivity filter. In the case of attraction, water would compete more strongly with ions for the space in the filter, and so the selective effects of excluded volume would be enhanced. If water were repelled from the filter, less repulsive selectivity would be expected. Again, (experimentally) appropriate selectivities could be produced by adjusting the volume of the filter of the model.

Our simulations were made using a specific representation of charged tethered groups and a particular estimate of the volume accessible to these groups but the simulations do not hinge on these choices. For instance, we could have represented larger parts of the DEKA sidechains by including neutral confined particles in the simulation, and increased the volume in which these groups are confined. Specifically, the relatively bulky sidechain of lysine could be modeled more realistically this way.[12]

The crucial parameter for a CSC mechanism as described here is the packing fraction of the ensemble of all atoms, mobile and structural, in the filter. The crowding of ions and protein atoms allow the finite size of the ions to determine selectivity. The mechanism does not require a specific geometry in which atomic positions and dimensions are strictly maintained.

4 Conclusions

Ion absorption has been computed for a model of the DEKA locus of biological Na channels in which mobile ions and charged structural groups are represented as charged hard spheres. The model channel selects Na^+ essentially by *excluding* larger monovalent cations while having a relatively weak affinity for Ca^{2+}. The presence of the positively charged lysine residue in the locus is essential for making the Na channel a ‘reluctant’ Ca channel. Excluded volume effects are essential for selecting small monovalent cations over large ones (CSC mechanism).

Acknowledgements

This work was supported by grants from the Hungarian National Research Fund (OTKA-F035222, to D.B.), DARPA (B.E., W.N.), NIH (Al 23007, to D.D.B.), and NSF (CHE98-13729, to D.H.). The authors thank Dr D. Gillespie for many useful comments and to Dr R. F. Rakowski for sharing results submitted for publication.

References

1 B. Hille, *Ionic Channels of Excitable Membranes*, Sinauer Associates, Inc., Sunderland, MA, 2001.
2 F. M. Ashcroft, *Ion Channels and Disease*, Academic Press, New York, 1999.
3 A. L. Hodgkin and A. F. Huxley, *J. Physiol. (London)*, 1952, **117**, 500.
4 D. A. Doyle, J. M. Cabral, R. A. Pfuetzner, A. Kuo, J. M. Gulbis, S. L. Cohen, B. T. Chait and R. MacKinnon, *Science*, 1998, **280**, 69.
5 H. R. Guy and S. R. Durell, in *Ion Channels and Genetic Diseases*, ed. D. Dawson, Rockefeller University Press, New York, 1995, pp. 1–16.
6 H. Terlau, S. H. Heinemann, W. Stühmer, M. Pusch, F. Conti, K. Imoto and S. Numa, *FEBS Lett*., 1991, **293**, 12.
7 J. Yang, P. T. Ellinor, W. A. Sather, J.-F. Zhang and R. W. Tsien, *Nature*, 1993, **366**, 158.
8 R. G. Tsushima, R. A. Li and P. H. Backx, *J. Gen. Physiol*., 1997, **109**, 463.
9 M. T. Perez-Garcia, N. Chiamvimonvat, R. Ranjan, J. R. Balser, G. F. Tomaselli and E. Marban, *Biophys. J*., 1997, **72**, 989.
10 S. H. Heinemann, H. Terlau, W. Stühmer, K. Imoto and S. Numa, *Nature*, 1992, **356**, 441.
11 I. Favre, E. Moczydlowski and L. Schild, *Biophys. J*., 1996, **71**, 3110.
12 Y.-M. Sun, I. Favre, L. Schild and E. Moczydlowski, *J. Gen. Physiol*., 1997, **110**, 693.
13 B. Hille, *J. Gen. Physiol*., 1971, **58**, 599.
14 B. Hille, *J. Gen. Physiol*., 1972, **59**, 637.
15 W. Nonner, L. Catacuzzeno and B. Eisenberg, *Biophys. J*., 2000, **79**, 1976.
16 W. Nonner, D. Gillespie, D. Henderson and B. Eisenberg, *J. Phys. Chem. B*, 2001, **105**, 6427.
17 D. Boda, D. D. Busath, D. Henderson and S. Sokołowski, *J. Phys. Chem. B*, 2000, **104**, 8903.
18 D. Boda, D. Henderson and D. D. Busath, *J. Phys. Chem. B*, 2001, **105**, 11 574.
19 D. Boda, D. Henderson and D. D. Busath, *Mol. Phys*., 2002, **100**, 2361.
20 D. Gillespie, W. Nonner and R. S. Eisenberg, *J. Phys.: Condens. Matter*, 2002 , in press.
21 J. G. M. Barthel, H. Krienke and W. Kunz, *Physical Chemistry of Electrolyte Solutions. Modern Aspects*, Steinkopff, Darmstadt, Springer, New York, 1998.
22 Y.-W. Tang, I. Szalai and K.-Y. Chan, *Mol. Phys*., 2001, **99**, 309.

23 Y.-W. Tang, I. Szalai and K.-Y. Chan, *J. Phys.Chem. A*, 2001, **105**, 9616.
24 Y. Yang, D. Henderson, P. Crozier, R. L. Rowley and D. D. Busath, *Mol. Phys.*, 2002, **100**, 3011.
25 G. Moy, B. Corry, S. Kuyucak and S.-H. Chung, *Biophys. J.*, 2000, **78**, 2349.
26 B. Corry, S. Kuyucak and S.-H. Chung, *Biophys. J.*, 2000, **78**, 2364.
27 W. N. Green, L. B. Weiss and O. S. Andersen, *J. Gen. Physiol.*, 1987, **89**, 841.
28 S. S. Garber and C. Miller, *J. Gen. Physiol.*, 1987, **89**, 459.
29 D. Naranjo and R. Latorre, *Biophys. J.*, 1993, **64**, 1038.
30 T. Begenesich and D. D. Busath, *J. Gen. Physiol.*, 1981, **77**, 489.
31 R. F. Rakowski, D. C. Gadsby and P. De Weer, *J. Gen. Physiol.*, 2002, **119**, 235.
32 B. Hille, *J. Gen. Physiol.*, 1975, **66**, 535.
33 A. Ravindran, H. Kwiecinski, O. Alvarez, G. Eisenman and E. Moczydlowski, *Biophys. J.*, 1992, **61**, 494.
34 D. Chen, L. Xu, G. Tripathy, G. Meissner and R. Eisenberg, *Biophys. J.*, 1997, **73**, 1337.
35 A. Ravindran, L. Schild and E. Moczydlowski, *J. Gen. Physiol.*, 1991, **97**, 89.
36 D. Gillespie and R. S. Eisenberg, *Eur. Biophys. J.*, 2002 , in press: DOI 10.1007/s00249-002-0239-x.
37 G. Eisenman, in *Ion-Selective Electrodes*, NBS Spec. Pub. 314, ed. R. A. Durst, National Bureau of Standards, Gaithersburg, MD, p. 1.
38 D. Goulding, J.-P. Hansen and S. Melchionna, *Phys. Rev. Lett.*, 2000, **85**, 1132.
39 D. Goulding, J.-P. Hansen and S. Melchionna, *Phys. Chem. Chem. Phys.*, 2001, **3**, 1644 [Links].
